Ferromagnetism-induced reentrant structural transition and phase diagram of the lightly doped insulator $La_{1-x}Sr_xMnO_3$ ($x \leqslant 0.17$)

H. Kawano
The Institute of Physical and Chemical Research (RIKEN), Wako, Saitama 351-01, Japan

R. Kajimoto, M. Kubota, and H. Yoshizawa
Neutron Scattering Laboratory, Institute for Solid State Physics, University of Tokyo, Shirakata 106-1, Tokai, Ibaraki 319-11, Japan

(Received 19 December 1995; revised manuscript received 22 February 1996)

The crystal structure of the lightly doped insulating system $La_{1-x}Sr_xMnO_3$ with $x \leqslant 0.17$ has been studied in detail using neutron diffraction. It has been established that this system has two orthorhombic phases. One is the O' phase with $b/\sqrt{2} < c < a$ and with static Jahn-Teller (JT) distortions, while the other is a pseudocubic phase with $b/\sqrt{2} \sim a \sim c$, which we call the O^* phase. In particular, the $x = 0.125$ sample exhibits $O^* \rightarrow O' \rightarrow O^*$ reentrant structural transitions. For $0.10 \leqslant x \leqslant 0.17$ a ferromagnetic ordering strongly suppresses lattice distortions at and below the ferromagnetic transition temperature. These results demonstrate a strong coupling between structural distortion, ferromagnetic ordering, and transport properties in the insulating $La_{1-x}Sr_xMnO_3$ system. [S0163-1829(96)50922-7]

Recent discoveries of a colossal magnetoresistance in distorted perovskite manganites,[1–8] a lattice structure switching by a magnetic field in the $La_{0.83}Sr_{0.17}MnO_3$,[9] and a charge ordered state controlled by a magnetic field in $Pr_{1/2}Sr_{1/2}MnO_3$ (Ref. 10) and in $Pr_{1-x}Ca_xMnO_3$ (Refs. 11–14) distinctly indicate that spin and lattice freedoms are intimately connected to transport properties in the doped manganate systems. These findings have renewed the interest in this family of manganites. One of the parent materials of these systems, $LaMnO_3$, is a Mott insulator. The substitution of a trivalent La ion by a divalent alkaline-earth ion leads to a ferromagnetic metallic state, which has been long known as a phenomenon mediated by a double exchange mechanism.[15–20] Another important feature of the manganites is that a Mn^{3+} ion is a Jahn-Teller (JT) ion. It has been recently pointed out that the influence of the JT effects has to be taken into account to understand the magnetic as well as transport properties in the lightly doped manganese system.[21,22]

Despite recent intense research activities in this field, there has been very little neutron diffraction work on the $La_{1-x}Sr_xMnO_3$ and $La_{1-x}Ca_xMnO_3$ systems since the early work of Wollan and Koehler on $La_{1-x}Ca_xMnO_3$.[16] Thus, motivated by the lack of detailed information on the magnetic and lattice structure of many of these manganites, we have carried out a systematic neutron diffraction study of the $La_{1-x}Sr_xMnO_3$ system in the insulating region with $x \leqslant 0.17$. In this paper we report the structural and magnetic phase diagrams of this system. The detailed magnetic behavior of the system has already been reported.[23]

The neutron diffraction measurements were performed using the triple axis spectrometers GPTAS, HER, and HQR installed at the JRR-3M reactor at JAERI, Tokai. The spectrometers were operated in the double axis mode, and the (002) reflection of pyrolytic graphite composite monochromators was utilized to obtain incident neutron wave vectors $k_i = 2.67$ Å^{-1} (GPTAS), 2.58 Å^{-1} (HQR), and 1.55 Å^{-1} (HER). A variety of collimator combinations were utilized as required by the measurements. The samples were placed in aluminum cells in a closed cycle helium gas refrigerator. The sample temperature ranging from 7 to 350 K was controlled within accuracy of 0.1°.

To accurately determine the structure of the $La_{1-x}Sr_xMnO_3$ samples and to avoid complications in the analysis due to the domain distribution and twinning, our measurements were performed on powder samples prepared by powdering melt-grown crystals. The method of sample preparation has been described in detail in Ref. 23. X-ray powder diffraction confirmed that all samples were single phase. In this paper, we labeled all samples by their nominal Sr concentrations.

First, we show the magnetic and structural phase diagrams of the lightly doped $La_{1-x}Sr_xMnO_3$ system in Fig. 1. In both panels, the filled symbols denote the data points determined by our group in this and previous works,[23,25] while the open symbols are taken from Ref. 8. The solid and dotted curves are guides to the eye.

The magnetic phase diagram is shown in the left panel; there are three magnetic phases, a paramagnetic (PM), a ferromagnetic (FM), and a canted antiferromagnetic (CAF) phase which are color-coded by blue, pink, and orange, respectively. We note that the low temperature phase for $0.10 \lesssim x \lesssim 0.15$ was identified as a ferromagnetic insulator phase in Ref. 8. Our neutron diffraction experiments,[23,25] however, have established that the samples with $x = 0.10, 0.125$ show two transitions, marking the onset of FM long-range ordering at T_c (filled squares) and AF ordering at T_{CA} (filled circles). Examining the temperature dependence of the resistivity measurements reported in Ref. 8, we find that the resistivity of these samples is metallic for $T_{CA} \leqslant T \leqslant T_c$, exhibits a sharp upturn at T_{CA}, and then becomes of semiconducting character. Therefore, we suggest

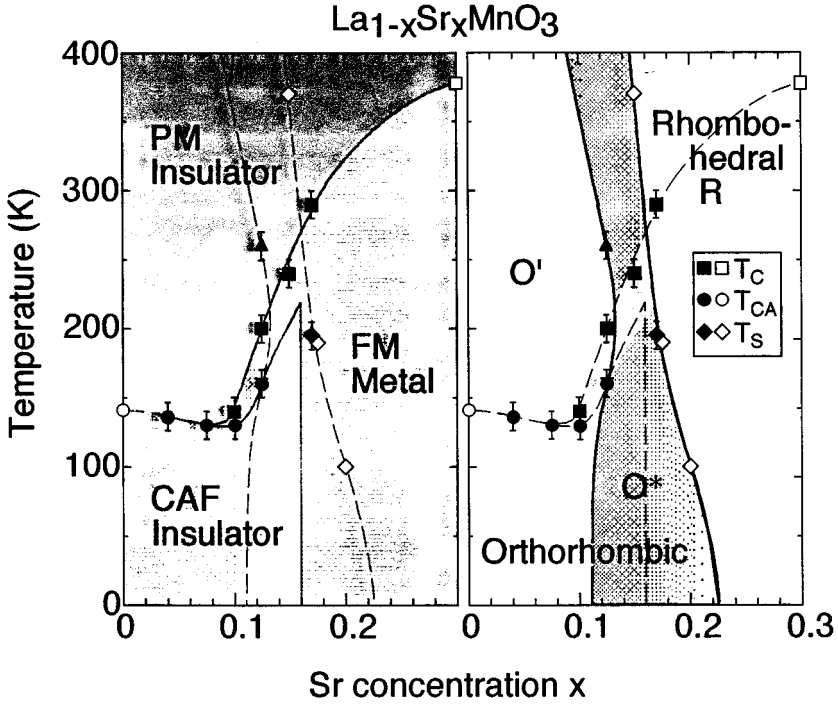

FIG. 1. Left panel: magnetic phase diagram of the insulating $La_{1-x}Sr_xMnO_3$ system with $x \leq 0.17$. Right panel: structural phase diagram. The squares and circles denote the onset of the ferromagnetic (FM) and antiferromagnetic (AF) components, respectively, while diamonds denote rhombohedral-to-orthorhombic phase transition temperatures. The triangles indicate the structural phase transitions observed in the $x=0.125$ sample. For explanation of the orthorhombic O' and O^* phases, see text.

that the intermediate phase for $T_{CA} \leq T \leq T_c$ is a FM metallic state, while the low-temperature phase is a CAF insulator as indicated in the left panel of Fig. 1.

The central results of the present study are summarized in the structural phase diagram shown in the right panel of Fig. 1. As described below, there are two orthorhombic phases. One is the well-known distorted-perovskite orthorhombic O' phase,[16] while we label the other as the O^* phase, which appears in the larger Sr concentration with $0.125 \lesssim x \lesssim 0.17$.

To examine the difference between the O' and O^* phases, the powder patterns were analyzed with use of a standard Rietvelt refinement program[24] and part of the results are summarized in Table I.[26] In the O' phase, the MnO_6 octahedra are largely distorted due to the static JT effect, and the lattice constants satisfy the relation $b/\sqrt{2} < c < a$. The O^* phase, on the other hand, is pseudocubic with $b/\sqrt{2} \sim a \sim c$, and the Mn-O bond lengths are almost equal, indicating that the O^* phase seems to lack a clear static JT distortion. One of the characteristic features of the distorted perovskite $GdFeO_3$ orthorhombic structure is the buckling of the MnO_6 octahedra along the b axis, where these tilt alternately closely towards the [001] direction. According to our analysis, both the O' and O^* phases show a clear buckling of the MnO_6 octahedra, indicating that both phases belong to the orthorhombic *Pbnm* symmetry. Nonetheless, the changeover between the two phases is accompanied with a clear phase transition as exemplified by the results of the $x=0.125$ sample.

Surprisingly, the $x=0.125$ sample shows $O^* \rightarrow O'$ and $O' \rightarrow O^*$ structural phase transitions with decreasing temperature (triangle symbols). Furthermore, distinct lattice distortions are observed for all FM-component-dominated samples with $0.10 \leq x \leq 0.17$ in the temperature range indicated by the purple-colored region right below T_c. In addition, there exists a rhombohedral (R) phase in the much higher doped region with $x > 0.17$. In contrast to the orthorhombic phase, the results of our analysis show that there is

TABLE I. Lattice parameters and Mn-O bond lengths for the insulating $La_{1-x}Sr_xMnO_3$ samples in the *Pnma* setting. O_x and O_z denote bond lengths within the ac plane, while O_y denotes those towards the b axis.

	x	T (K)	a (Å)	$b/\sqrt{2}$ (Å)	c (Å)	O_x (Å)	O_y (Å)	O_z (Å)
O'	0.0	200	5.727(1)	5.433(1)	5.529(1)	1.91(3)	1.97(1)	2.18(2)
	0.04	200	5.697(1)	5.451(1)	5.547(1)	1.91(2)	1.97(1)	2.16(2)
	0.075	200	5.611(1)	5.451(1)	5.538(2)	1.90(5)	1.97(1)	2.12(4)
	0.10	200	5.586(1)	5.455(1)	5.540(1)	1.91(5)	1.97(1)	2.09(4)
	0.125	210	5.561(2)	5.489(1)	5.556(2)	2.0(1)	1.99(2)	2.0(1)
O^*	0.125	30	5.532(4)	5.522(3)	5.536(3)	2.0(2)	2.01(3)	2.0(2)
		300	5.537(3)	5.530(3)	5.545(2)	2.0(2)	2.02(3)	2.0(2)
	0.15	209	5.479(3)	5.511(2)	5.517(2)	1.9(1)	2.02(2)	2.0(1)
	0.17	150	5.473(2)	5.490(2)	5.524(2)	1.96(8)	1.99(2)	1.96(8)
R	0.17	210	5.522(1)		13.347(3)	1.97(1)	1.97(1)	1.97(1)

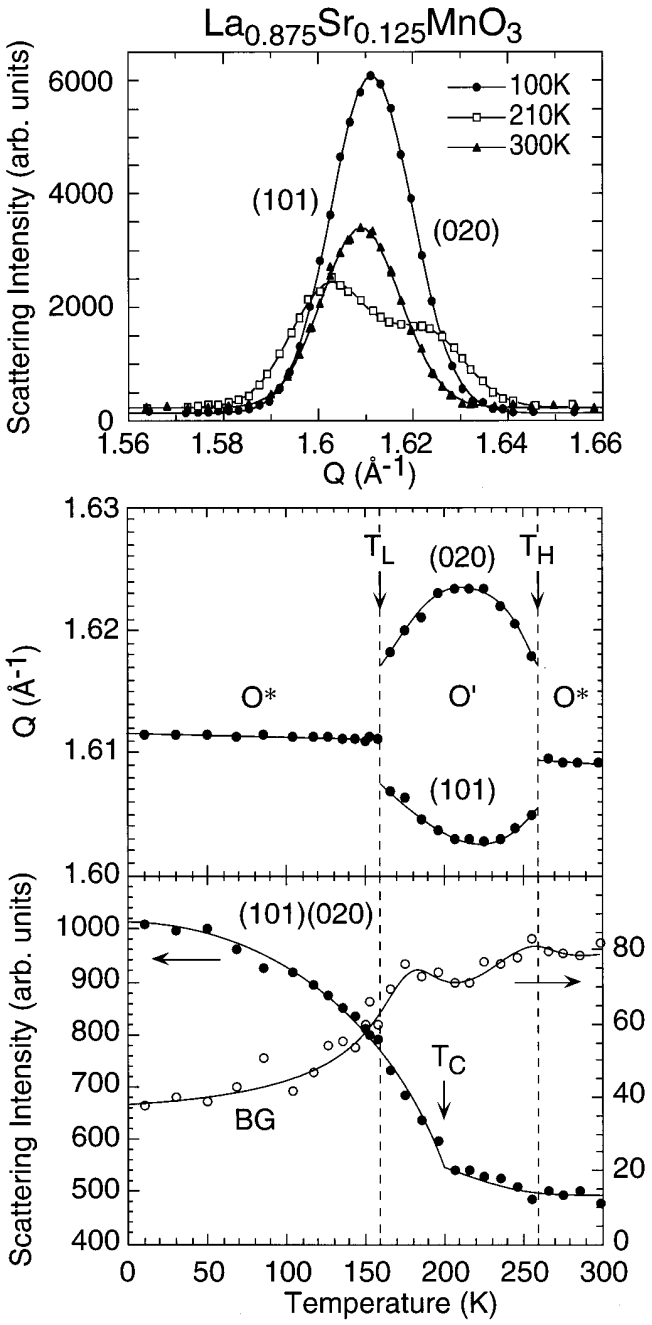

FIG. 2. Results of the $La_{0.875}Sr_{0.125}MnO_3$ sample. Top panel: Temperature dependence of the profiles of the (101) and (020) reflections. Middle panel: Temperature dependence of the peak positions of the (101) and (020) reflections. Bottom panel: Temperature dependence of the integrated intensities of the (101) and (020) reflections and the background scattering.

no buckling in the R phase, and the three Mn-O bonds lengths become identical.

We now describe the behavior of each concentration in detail. The most striking and interesting behavior was seen in the $x=0.125$ sample, and the results are shown in Fig. 2. The top panel shows the profiles of the (101) and (020) reflections measured at 300, 210, and 100 K, respectively. The profiles at 300 and 100 K are single peaks, reflecting that the $x=0.125$ sample is in the O^* phase, while the profile at 210 K clearly splits into two peaks, indicating a transition to the O' phase. This drastic change of profiles is due to the successive structural phase transitions ($O^* \rightarrow O' \rightarrow O^*$). The middle panel shows the shift of peak positions as a function of temperature. The $x=0.125$ sample undergoes a structural phase transition from the O^* phase to O' phase at $T_H=260$ K. Then, with decreasing temperature, the single peak splits into two peaks at T_H and their splitting gradually increases. This means that the decrease of temperature favors larger JT distortions, and stabilizes the O' phase. With further decreasing temperature, however, the two peaks start to approach each other below ~ 200 K, and suddenly recover the single peak structure at $T_L=160$ K. To examine the origin of these changes, the temperature dependences of the integrated intensity of the (101) and (020) peaks and that of background scattering were measured and the results are depicted at the bottom panel of Fig. 2. The $x=0.125$ sample exhibits FM ordering below $T_c=200$ K. By comparing it with the middle panel, it is clear that the decrease of the splitting of two peaks coincides with the onset of the FM long-range order. The FM component drastically suppresses the static JT distortion and even leads the $x=0.125$ sample to a reentrant structural transition.

One can clearly see similar anomalies in all the FM-component-dominated samples, although the behavior is less dramatic. The behavior of the $x=0.10$, 0.15, and 0.17 samples is shown in Fig. 3. The left column in this figure shows the temperature dependence of the peak positions of the (101) and (020) reflections, while the right column gives the temperature dependence of the integrated intensity and that of background scattering. The magnetic ordering temperatures of the three samples are indicated by arrows. As seen in the right column, all three samples show a sharp increase of the integrated intensity and a decrease of background scattering below T_c. On the other hand, from the left column, it is evident that three samples exhibit anomalous shifts of peak positions in a limited temperature range just below T_c. For the $x=0.17$ sample we also show the temperature dependence of the (102) and (201) nuclear Bragg reflections which are allowed only in the orthorhombic structure. The $x=0.17$ sample undergoes a R-to-O^* structural phase transition at $T_s \sim 195$ K, although this transition has little effect on the temperature dependence of peak shift. Note that the correct index of the reflection in the rhombohedral phase is (102) instead of (101) and (020) for the orthorhombic phase.

It is also interesting to point out that the peak shift ΔQ is largest in the $x=0.125$ sample, and as the concentration deviates from $x=0.125$, the shift ΔQ diminishes rapidly as seen in Figs. 2 and 3. It should be noted that $x=0.125$ is a commensurate value which should be expected to favor a particular type of charge ordering as in the compounds with $x=1/3, 1/2$. The facts that ΔQ is maximum at $x=0.125$ and that the sample shows a first-order phase transition at T_L strongly suggest the existence of such a particular type of charge ordering. It is well known that one of the high-T_c layered cuprates, $La_{2-x}A_xCuO_4$, shows successive structural phase transitions, and a 1/8 charge-ordered phase at $x=0.125$ suppresses superconductivity.[27] It is evident that a 1/8 charge order also plays a crucial role in the present system.

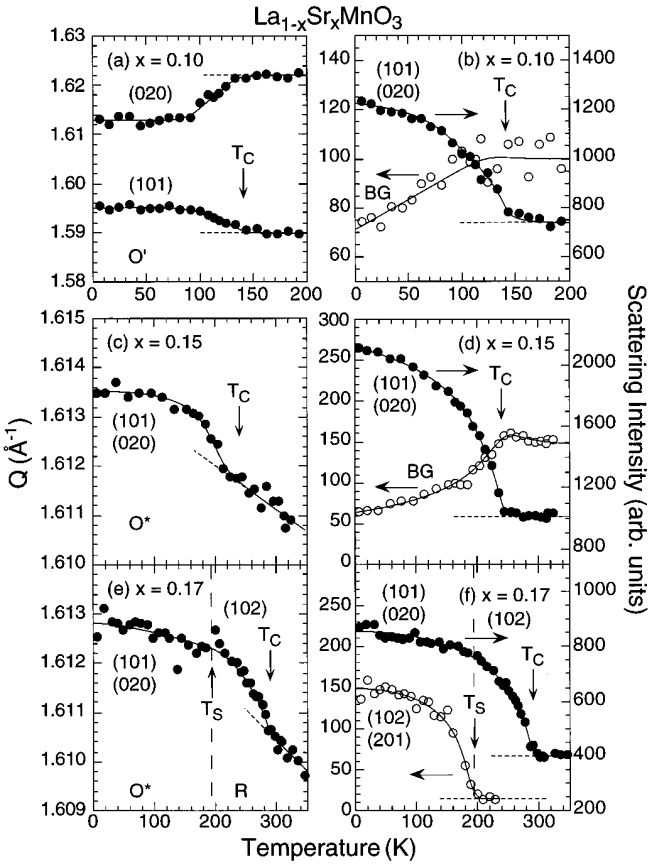

FIG. 3. Left column: Temperature dependence of the peak positions of the (101) and (020) reflections for the $x=0.10$, 0.15, and 0.17 samples. Right column: Temperature dependence of the integrated intensities of the (101) and (020) reflections. The open symbols in the top and middle panel give the temperature dependence of background intensity, while those in the bottom panel depict the temperature dependence of the superlattice reflections (102) and (201) in the orthorhombic O^* phase in the $x=0.17$ sample.

As mentioned above, there is a strong correlation between resistivity and magnetism in this system. The resistivity of the $x=0.10$ and 0.15 samples shows a drastic drop at T_c, and then shows a sharp upturn at a lower temperature.[7,8] The onset of the FM long range ordering in this system leads to a drastic drop of resistivity, and causes a release of lattice distortions. Such behavior can be interpreted as follows. The FM component activates the double exchange mechanism, giving rise to a metallic temperature dependence of the resistivity. In the FM phase, a strong electron-phonon coupling in the system favors a gain of kinetic energy of e_g electrons against an energy gain associated with a JT distortion. Therefore, the system releases JT distortion, increasing the Mn-O bond angle, and resulting in larger matrix elements of electron hopping between Mn sites.

We believe that the upturn of resistivity corresponds to the onset of the AF component T_{CA}. Specifically for the $x=0.125$ sample, this upturn also coincides with the lower structural transition temperature T_L. Unfortunately, the temperature dependence of the resistivity of the $x=0.125$ sample was not reported in Refs. 7 and 8. Nevertheless, we can have a reasonable prediction based on the present observations. The resistivity should show a small increase of slope at the O' to O^* transition at T_H, a rapid decrease at and below T_c, and a sharp first-order-like upturn at T_{CA}.

We finally point out that an insulator-metal phase boundary for the $La_{1-x}Sr_xMnO_3$ system is actually located at $x\sim 0.10$, but the AF component suppresses the metallic state below T_{CA} for the samples with $0.10\leqslant x\leqslant 0.15$ as shown in the phase diagram of Fig. 1.

In summary, we have carried out neutron diffraction experiments on the lightly doped insulating system $La_{1-x}Sr_xMnO_3$ with $x\leqslant 0.17$, and have established its correct phase diagram. There are two orthorhombic phases, an O' phase with a static JT distortion and an O^* phase with no static JT distortion. All FM-component-dominated samples show anomalous peak shifts in a limited temperature range right below T_c. These results are clear manifestations of the coupling among the lattice, magnetism, and transport phenomena in the insulating $La_{1-x}Sr_xMnO_3$ system. A study of a possible charge ordering in the $x=0.125$ sample is now in progress.

We thank J. A. Fernandez-Baca for a critical reading of the manuscript. This work was supported by the Special Researcher's Basic Science Program (RIKEN) and by a Grant-In-Aid for Scientific Research from the Ministry of Education, Science and Culture, Japan.

[1] R. M. Kusters *et al.*, Physica B **155**, 362 (1989).
[2] K. Chabara *et al.*, Appl. Phys. Lett. **63**, 1990 (1993).
[3] R. von Helmont *et al.*, Phys. Rev. Lett. **71**, 2331 (1993).
[4] S. Jin *et al.*, Science **264**, 413 (1994).
[5] H. L. Ju *et al.*, Appl. Phys. Lett. **65**, 2108 (1994).
[6] M. McCormack *et al.*, Appl. Phys. Lett. **64**, 3045 (1994).
[7] Y. Tokura *et al.*, J. Phys. Soc. Jpn. **63**, 3931 (1994).
[8] A. Urushibara *et al.*, Phys. Rev. B **51**, 14 103 (1995).
[9] A. Asamitsu *et al.*, Nature (London) **373**, 407 (1995).
[10] Y. Tomioka *et al.*, Phys. Rev. Lett. **74**, 5108 (1995).
[11] Y. Tomioka *et al.*, Phys. Rev. B **53**, R1689 (1996).
[12] Y. Tomioka *et al.*, J. Phys. Soc. Jpn. **64**, 3626 (1995).
[13] H. Yoshizawa *et al.*, Phys. Rev. B **52**, R13 141 (1995).
[14] H. Yoshizawa *et al.*, J. Phys. Soc. Jpn. **65**, 1043 (1996).
[15] G. H. Jonker and J. H. van Santen, Physica **16**, 337 (1950).
[16] E. O. Wollan and W. C. Koehler, Phys. Rev. **100**, 545 (1955).
[17] G. H. Jonker, Physica **22**, 707 (1956).
[18] C. Zener, Phys. Rev. **82**, 403 (1951).
[19] P. W. Anderson and H. Hasegawa, Phys. Rev. **100**, 675 (1955).
[20] P.-G. de Gennes, Phys. Rev. **118**, 141 (1960).
[21] A. J. Millis *et al.*, Phys. Rev. Lett. **74**, 5144 (1995).
[22] A. J. Millis *et al.* (unpublished).
[23] H. Kawano *et al.*, Phys. Rev. B **53**, 2202 (1996).
[24] Y.-I. Kim and F. Izumi, J. Ceram. Soc. Jpn. **102**, 401 (1994).
[25] H. Yoshizawa *et al.* (unpublished).
[26] Detailed analysis of powder patterns observed with better angular resolution will be reported separately.
[27] J. M. Tranquada *et al.*, Nature (London) **375**, 561 (1995).